

Optimization of photovoltaic provision in a three-dimensional city using real-time electricity demand

Rui Zhu ^{a,b,c}, Cheng Cheng ^{d,e,*}, Paolo Santi ^{f,g}, Min Chen ^{h,i,j}, Xiaohu Zhang ^a, Martina Mazzarello ^f, Man Sing Wong ^{b,c}, Carlo Ratti ^f

^a Senseable City Laboratory, Future Urban Mobility IRG, Singapore-MIT Alliance for Research and Technology, 1 Create Way, 09-02 Create Tower, Singapore 138062, Singapore

^b Department of Land Surveying and Geo-Informatics, The Hong Kong Polytechnic University, Hong Kong, China

^c Research Institute for Land and Space, The Hong Kong Polytechnic University, Hong Kong, China

^d School of Transportation, Southeast University, Nanjing, Jiangsu, 211189, China

^e Department of System Science, Institute of High Performance Computing, Agency for Science, Technology and Research (A*Star), 1 Fusionopolis Way, #16-16 Connexis, Singapore 138632, Singapore

^f Senseable City Laboratory, Department of Urban Studies and Planning, Massachusetts Institute of Technology, Cambridge, MA 02139, USA

^g Istituto di Informatica e Telematica del CNR, 56124 Pisa, Italy

^h Key Laboratory of Virtual Geographic Environment (Ministry of Education of PR China), Nanjing Normal University, Nanjing, 210023, China

ⁱ State Key Laboratory Cultivation Base of Geographical Environment Evolution (Jiangsu Province), Nanjing, 210023, China

^j Jiangsu Center for Collaborative Innovation in Geographical Information Resource Development and Application, Nanjing, 210023, China

ARTICLE INFO

Keywords:

Solar energy
Solar urban planning
Spatial optimization
Big data computation
Geographic information systems
3D cities

ABSTRACT

Promoting the use of solar photovoltaic (PV) systems in global cities can be an effective way to cope with severe environmental problems caused by the consuming of fossil fuels. However, a complex urban environment challenges the effective use of PV systems for practical applications. Essentially, this is a spatial optimization problem, where the goal is maximizing the harvesting of solar energy while minimizing occupied urban surfaces. To address this problem, this paper proposes three hierarchical optimizations. First, computational optimization provides a parallel architecture for an established 3D solar estimation model to achieve spatially scalable computation with high spatio-temporal resolution. Second, priority optimization determines the use of different urban partitions considering various constraints. Third, capacity optimization analyzes the spatial and quantitative distribution of solar potential, constrained by the smallest solar irradiation and the minimum surface area to be used. The overall optimization framework is then set to obtain the minimum PV installation capacity required to meet the real demand with the identification of urban surfaces to be equipped with PV modules. By using smart meter data with high temporal resolution in the city of Bologna, Italy, our analysis not only provides executable plans to meet the real demand but also reveals that rebalance and storage capacity are needed to achieve a real-time self-supportive architecture. The proposed analytic and optimization framework can promote distributed PV systems in urban areas and facilitate energy transition adapted to a variety of applications.

1. Introduction

1.1. Background and motivation

Cities consume 60% to 80% of global energy that accounts for more than 70% of global greenhouse gas emissions [1], which exacerbates global warming and air pollution [2,3] and makes the urban heat island effect severe [4–6]. To tackle this problem, one possible solution is promoting photovoltaic (PV) systems to generate green electricity

with significant reduction of carbon emission [7–9]. Compared with utility-scale solar power plants which are usually located in remote and bare lands to provide a stable fuel price, distributed generation in cities has been booming for its potential to provide a self-supportive system [10,11]. By equipping PV modules on rooftops, ground, and even façades, and connecting them to the local utility distribution grid [12], it is in principle possible to form nearly self-sufficient small-scale systems, significantly reducing the costs related to

* Corresponding author at: Department of System Science, Institute of High Performance Computing, Agency for Science, Technology and Research (A*Star), 1 Fusionopolis Way, #16-16 Connexis, Singapore 138632, Singapore.

E-mail address: cheng_cheng@ihpc.a-star.edu.sg (C. Cheng).

transporting energy, as well as increasing resilience of the energy grid. To achieve this vision and propose an executable plan for distributed PV generation, two components are required: (i) an accurate estimation of solar PV potential on large three-dimensional (3D) urban surfaces to determine solar abundant locations, and (ii) optimization of solar PV capacity to meet the real electricity demand. This is important for smart grid operators who need to plan the PV installation capacity and location based on the techno-economic assessment that considers the feed-in tariffs initiatives, the installation cost, and the operation and maintenance cost, which can affect the economic performance of distributed PV systems significantly [13–15].

However, there is a challenge for solar estimation in a complex urban environment since the spatio-temporal distribution of solar irradiation is significantly influenced by urban morphology, such as massing [16], density [17,18], and orientation of buildings [19], and even terrain variation [20]. To overcome the challenge, several studies have proposed various solar estimation models, either focusing on rooftops [21–24], façades associated with rooftops [25–28] or ground [29], or all the three partitions [30,31]. However, these models lack spatial scalability that cannot support an estimation over large urban areas with a fine spatio-temporal resolution, which is a crucial component to design distributed PV systems in cities. Addressing this challenge is thus the first research objective of this paper.

Besides estimating urban PV potential, planning PV systems at solar abundant urban space is the other important issue. One study investigated the characteristics of machine learning-based PV panel segmentation, which offers a cost-effective and data-consistent method for estimating the existing PV installed capacity [32]. In comparison, our study aims at proposing an executable plan for distributed PV power generation on an existing built environment, which will achieve a balance between the demand for electricity and the supply of solar energy. To develop energy-efficient cities, some studies have already proposed PV plans by investigating the relationship between electricity demand and supply either based on a theoretical model [33,34] or estimated demand [35]. However, they have not addressed the spatial optimization that maximizes the solar PV potential with a minimal number of urban surfaces occupied to meet the electricity demand. Addressing this issue becomes our second research objective.

1.2. Modeling of a three-dimensional solar city

It is vital to accurately estimate PV potential on urban envelopes to utilize solar energy effectively. One method consists in estimating sky view factors [36,37], which is constrained to work only for particular streets which had been captured by street-view images. Also, irradiations on building surfaces cannot be derived. Another approach consists in estimating the potential on rooftops only, which were mostly utilized in cities [22–24]. Meanwhile, two studies incorporated extreme weather events and cloud cover into the planning of urban energy systems [38] and the estimation of PV potential on rooftops [24], respectively. Specifically, one established a probability distribution map of annual cloud cover for PV potential estimation [24], since cloud cover can substantially impact the received irradiations even if two cities are at the same latitude and have similar urban morphology. Our study will also consider this effect by incorporating historical cloud cover data into the determination of atmospheric conditions reliably.

In vertical cities, façades can also be optimal locations for semitransparent PV modules to save urban space and generate electricity [25–29]. In addition, being used as an alternative to conventional window glass, the use of semitransparent PV allows a lower amount of solar irradiation to penetrate the indoor environment, which thus provides moderate daylighting and reduces the use of air conditioners during the summer. Thus, the use of PV on façades can be especially useful in cities with temperate to warm climates. In this field, one study incorporated the effect of greenery in the estimation of solar irradiation on the built environment [39], which cannot be ignored in urban areas where trees

are an important component of the urban landscape. In the case under our study with an urban area in the city of Bologna, Italy, the effect of trees is marginal since greenery is a minority in the study area.

Further studies suggested that their models were able to estimate PV potential on the entire urban envelopes, including rooftops, ground, and façades [30,39–42]. For example, by incorporating an established model [43] into the development of the SORAM model [41], one study proposed a ray-tracing algorithm to determine the intersection between 3D ray vectors and an entity to calculate solar potentials on urban surfaces. However, the capability of applying the method on an area having a large number of buildings is not reported, and the ability to account for complex building geometries with concave and nested polygon footprints is uncertain as well.

Previous work developed a model that created 3D shadow surfaces associating at the corresponding façades and then made 3D intersection between the shadow surfaces and other building surfaces, which thus generated 3D intersection lines that divide shadow from light [30]. Furthermore, 3D point clouds which are used to present urban envelopes were considered to be in light when they are above the intersection lines so that the points are assigned to the specified irradiation. The 3D intersection essentially considers the shadow effect made by surrounding or even distant building blocks. Therefore, the model is expected to satisfy the computation need of our study. However, the introduced 3D intersection method potentially creates largely redundant computation; for instance, all ground points will be retrieved while only a small proportion of them is in the shadow at noon. To address this problem, our study aims to propose a parallel computational architecture with acceleration techniques implemented in a spatial database management system to speed up computation and enable the application of the model to a large urban area. Most importantly, the previous models have not developed a spatially scalable computational framework, which means that parallel computing for spatial-contiguous regions and for a series of time intervals is not supported, even using the most advanced central processing units. Overcoming this challenge is crucial for smart grid operators to detect suitable PV locations with abundant solar potential so that global optimization of the PV installation capacity can be achieved over a large urban area to meet the electricity demand.

1.3. Solar urban planning

Previous studies on the planning of solar-related applications can be categorized into three classes: solar changes on the existing buildings over different spatial and temporal scales [25,39,40,44]; solar transformation when cities reform from the current urban form to the future urban landscape based on a determined master plan [31]; and solar optimization by designing new urban forms or hybrid systems [45,46]. However, studies focusing on existing buildings investigated changes of irradiation either at a coarsely spatial resolution by aggregating a cluster of buildings [44] or a coarsely temporal resolution in monthly or seasonal scales [25,39,40]. Different from these studies, our study will optimize the PV planning strategy by considering different scenarios in a complex urban environment and develop a spatio-temporal data analytic method to reveal the spatial and quantitative distribution patterns of solar PV potential on detailed 3D urban envelopes, which is crucial for planning PV systems with abundant solar energy.

To achieve the second objective of maximizing solar harvesting and minimizing occupied urban surfaces, it is crucial to perceive both electricity demand and solar potential with high spatio-temporal granularity and to combine that into an optimization framework. Even though a recent study has stated that they estimated solar energy at a fine spatial and temporal resolution covering the entire Arabian Peninsula [47], it is still inappropriate to be used for cities, where a microscopic investigation is needed within a scale of meters and hours, respectively. With a similar research objective on solar urban planning, another study investigated the impacts of nine types

of urban morphology on the energy demands, introduced the urban cell concept, and used a game-theoretic approach to optimize energy systems and electricity networks between the urban cells [48]. The results suggested that it can improve the installed renewable energy and the net present value considerably. In comparison, our study will propose spatial optimization aiming for the maximized PV installed capacity and minimized urban occupation to meet the real electricity demand. To solve the high granular optimization of PV capacity and location, a possible way is to combine estimation of demand with smart meters which provide accurate and reliable electricity demand with high spatial (e.g., in meters) and temporal (e.g., in minutes) resolutions, with an estimation of supply derived from 3D solar irradiation models. As it is rare to find studies incorporating smart-meter data into spatial optimization of distributed PV systems, one of the contributions of this study is that we are from a technical and empirical perspective to demonstrate planning of PV installation capacity for near-real-time electricity demand.

1.4. Contribution

To sum up, the originality of this study is three-fold: (i) optimizing the computational framework by proposing a parallel computation architecture to allow spatial scalability of a 3D solar estimation model and global optimization of the PV installation capacity over a large urban area; (ii) optimizing the priority of utilizing different urban partitions for multi-scenario solar harvesting constrained by land use and urban landscape; and (iii) optimizing the PV installation capacity by maximizing solar harvesting while minimizing urban surface occupation to meet real electricity demand.

The rest paper is organized as follows. Section 2 proposes a PV provision optimization framework consisting of three hierarchical layers, i.e., the computation optimizations, the usage priority optimization of urban partitions, and the PV installation capacity optimization. Furthermore, as an empirical investigation, Section 3 presents the study area and data collection. Section 4 demonstrates the results to supply real-time electricity demand. Finally, Section 5 makes discussion and conclusion.

2. Optimization of equipping PV modules

2.1. Optimization framework

The methodology for planning PV modules is composed of three hierarchical optimization steps (Fig. 1). First of all, computation optimization will be used by incorporating a solar estimation model [30, 31] to achieve spatially scalable computation by utilizing multiple threads if the study area has a large number of buildings. Then, the priority of using three urban partitions (i.e., rooftops, façades, and the ground) will be optimized, constrained by land use and urban landscape. Finally, the PV installation capacity and location will be optimized to meet the real demand by maximizing the solar harvesting and minimizing the occupation of urban surfaces, which is supported by the spatio-temporal statistics that reveal the spatial distribution of solar irradiation and the quantitative distribution of the generated electricity.

2.2. Modeling solar irradiation on urban envelopes

The study utilizes an established model to estimate solar irradiation on three-dimensional (3D) urban envelopes [30,31]. Based on footprints of buildings associated with the height attribute, the model constructs urban envelopes as a set of 3D polygons denoted by \mathcal{G} , which can be decomposed as rooftops \mathcal{O} , façades \mathcal{F} , and ground \mathcal{D} . Given this, each element $g \in \mathcal{G}$ can be discretized using a set of homogeneous grids with a constant resolution d , which are spatially contiguous with each other. Then, centroids denoted by \mathcal{P} can be extracted from the grids to present 3D point clouds of the urban envelopes. More specifically,

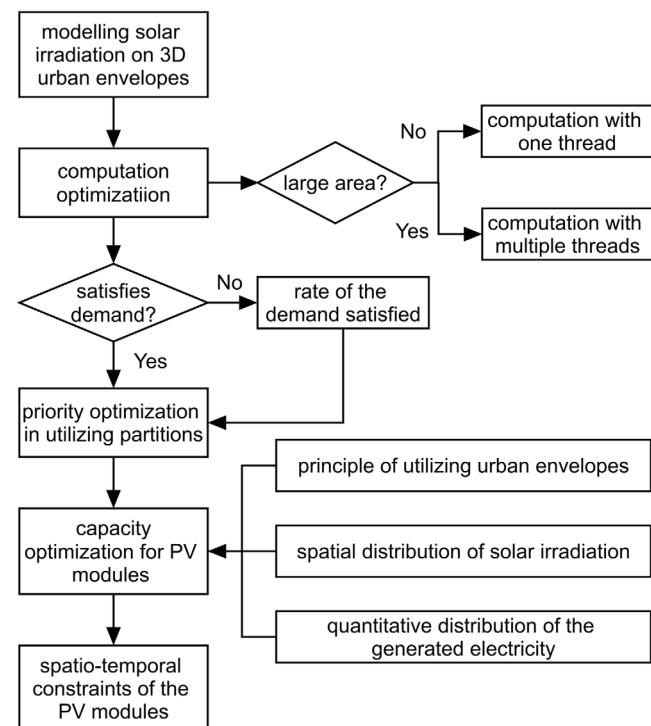


Fig. 1. The framework contains three hierarchical optimizations for planning deployment of PV modules.

$\forall p \in \mathcal{P}$, p is described by the unique ID id , the 3D coordinate l on surface of g , and the irradiation u . Next, a complete set of parallel solar irradiations passing through the atmosphere and arriving at the point clouds \mathcal{P} are determined and denoted by $\mathcal{R} = \{r\}$. Furthermore, the 3D intersection between façades \mathcal{F} and irradiations \mathcal{R} can be made to produce the set of 3D shadow surfaces denoted by \mathcal{S} , which is hence modified as \mathcal{S}' because (i) solar-facing façades will not make a shadow surface, (ii) coincident façades with a lower height will not make a shadow surface either, and (iii) nearby buildings and concave rooftops may reshape the original shadow surfaces. Finally, $\forall p \in \mathcal{P}$, irradiation u is set to 0 if it is below the shadow line \mathcal{S}' , and $u = f(u_o)$ if it is above \mathcal{S}' .

2.3. Computation optimization with a parallel architecture

The model was implemented as hierarchical SQL functions in a relational database management system (DBMS) of PostgreSQL 11 with the support of PostGIS 2.5. Even though the model has introduced three accelerating technologies (i.e. spatial indexing, replacing large tables for UPDATE queries, and creating temporary tables in RAM) to achieve fast computation, it is still a challenge to achieve parallel computation by invoking multiple threads in PostgreSQL 11 as execution plans may vary when the table size changes, which usually happens when estimating solar irradiation at different hours of a day.

To address the challenge of parallel computation in a DBMS, we propose a simple and effective parallel computational framework based on four hierarchical structures. First, the entire area to be estimated is defined as a 100 m outer buffer of the study area to get rid of the marginal effect. This is done using a set of sub-areas with a 100 m overlap (Fig. 2) so that each one can be computed in parallel in a series of independent databases. This way, the computational load in each database can be reduced dramatically. For example, millions of intermediate records generated from the intersection between solar irradiations \mathcal{R} and 3D urban envelopes \mathcal{G} may perform a 75% reduction when the computational area becomes one-fourth of the original. Then,

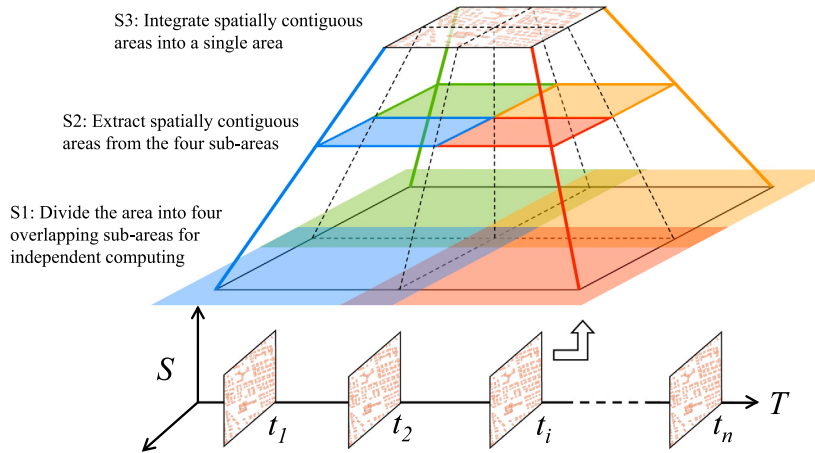


Fig. 2. The framework of parallel computation based on discretizing the study area into overlapping sub-areas.

spatially contiguous areas can be extracted from all the sub-areas with 3D point clouds having obtained qualified solar irradiation. After that, the sub-areas are integrated and reformed as the original study area, which has obtained solar irradiation \mathcal{R} at time t_i . Finally, a set of the above architectures can be built up to compute solar irradiation on an annual basis \mathcal{T} concurrently.

2.4. Priority optimization in utilizing different partitions

This study defines solar irradiation as a tuple $r = \langle e, z, t, l, u_o \rangle$, meaning that the irradiation comes from the atmosphere at an elevation e and an azimuth z with qualified irradiation u_o and arrives on an urban surface locating at a 3D coordinate l at time t . To utilize solar energy in a city, we prefer an area having $\{u\}$ that is spatially concentrated and quantitatively large. Notably, u may not equal u_o since an urban surface g may not have a vertical angle with r all the time so a transformation is needed according to the energy conservation law. Thus, the principle is to maximize the sum of u given a minimized sum of the usable area a , where u is at least equal to or larger than u_{use} . More formally:

$$U = \max(\sum u) \mid (u \geq u_{use} \wedge A = \min(\sum a)) \quad (1)$$

The above function is constrained by different concerns when it is applied to urban envelopes that are partitioned into rooftops, façades, and ground surfaces. To save land-precious urban areas, people prefer to use building surfaces for distributed generation, such as houses in communities and skyscrapers in urban areas. As a driven factor of obtaining U , it is reasonable to utilize urban envelopes in order of façades/rooftops and ground determined by specific geo-location. For instance, cities located at low latitudes (e.g., Singapore) prefer rooftops, while façades overtake rooftops for high latitude cities (e.g., Stockholm). However, the concern changes in a different situation. For historical cities with a rich architectural landscape (e.g., Bologna, Stockholm, and Barcelona), extensively utilizing façades and rooftops will cause remarkable destruction of the original landscape. Because of this reason, a convincing way is assigning the highest priority to free space on the ground followed by rooftops and finally façades, which brings an additional benefit of easing PV maintenance. We tend to use rooftops more than façades because rooftops will make less influence on the landscape, considering a possible scenario that façades are covered by a large area of PV modules. Nevertheless, it may still be a challenge if the occupation of the ground is significantly large, especially in land-precious urban areas. In this consideration, we make a trade-off that rooftops, ground, and façades are used as a decreasing priority (Table 1).

Table 1

Three concerns leads to four different proprieties to equip PV modules on urban envelopes.

| No. | Concerns | 1st priority | 2nd priority | 3rd priority |
|-----|-------------------------|--------------|--------------|--------------|
| 1 | Efficiency (high lati.) | Façades | Rooftops | Ground |
| 2 | Efficiency (low lati.) | Rooftops | Façades | Ground |
| 3 | Landscape | Ground | Rooftops | Façades |
| 4 | Trade-off | Rooftops | Ground | Façades |

2.5. Capacity optimization for PV modules

As previously discussed, solar farming prefers surfaces that have both spatially concentrated and quantitatively large irradiation. Therefore, explicitly understanding the spatial distribution of solar irradiation is imperative to determine usable surfaces. We expect to utilize solar irradiation u which is equal to or larger than a threshold $x \cdot u_m$, where u_m is the maximum irradiation on an urban partition (i.e., rooftops, façades, or ground) and x is the proportion of u_m . Hence, it computes the rate of usable area $p(a)$ for each surface:

$$p(a) = \frac{a_{use}}{a_{sur}} \mid u \geq x \cdot u_m \quad (2)$$

Then, it summarizes the rate of urban surfaces $p(s)$ that satisfies $p(a)$ during a period, which is an empirically cumulative distribution equaling the number of usable surfaces n_{use} divided by the sum of the surfaces n_{sum} in one partition:

$$p(s) = \frac{n_{use}}{n_{sum}} \mid p(a') \geq p(a) \quad (3)$$

Furthermore, the total supply $s(e)$ can be estimated by summarizing generated electricity for a given x , the proportion of u_m . Next, the smallest x can be determined by comparing $s(e) = r \sum u$ with the real demand, where r is the photoelectric conversion efficiency. It corresponds to the smallest occupation of urban surfaces for PV modules. Notably, the occupied area varies across different concerns if the first priority has already satisfied the demand. Also, more partitions are needed if the first priority cannot meet the demand, which will utilize urban envelopes comprehensively.

3. Empirical investigation

3.1. Study area

As one of the most well-preserved historical cities across the world, the city of Bologna in Italy attracted more than three million overnight-stay tourists in 2019 [49]. Thus, it is especially important to reduce

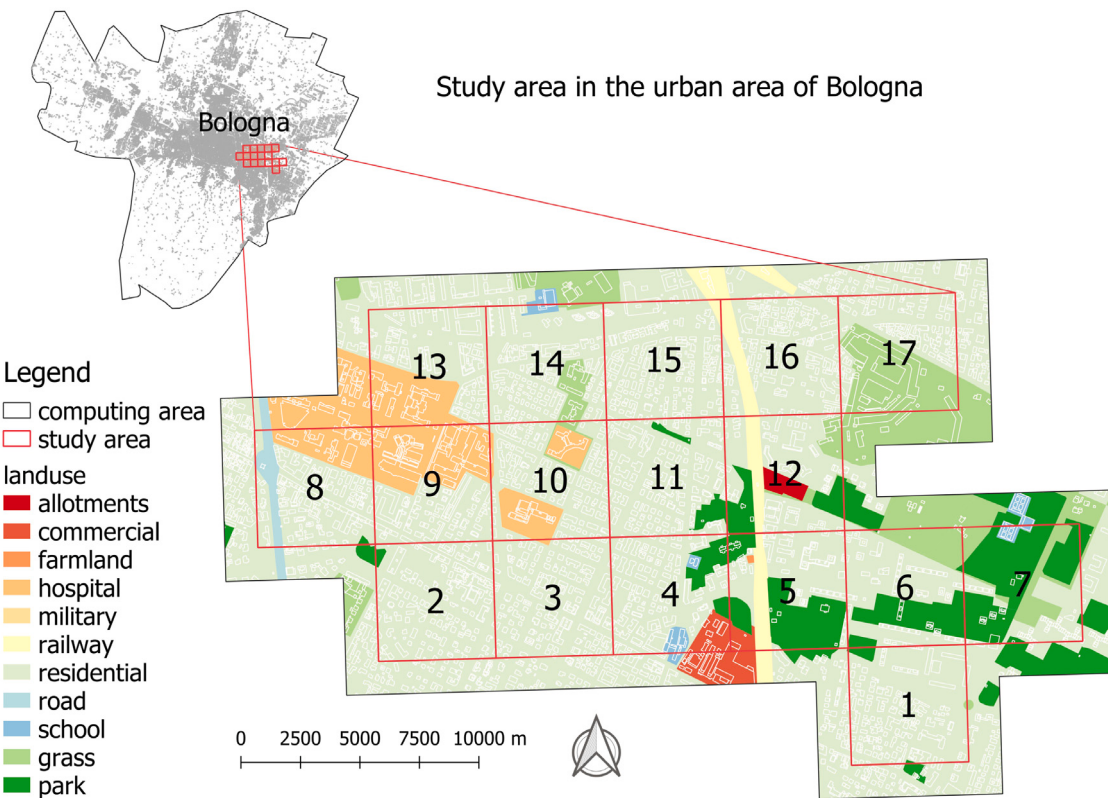


Fig. 3. The study focuses on an urban area next to the old city center in Bologna, which is discretized as seventeen grid cells having red boundaries.

greenhouse gas emissions in the city for environmental protection and preserving historic buildings. Bologna has signed the Covenant of Mayor's initiative to achieve a reduction of greenhouse emissions at 20% by 2020 and 40% by 2030 [50]. Thus, it is reasonable to promote distributed PV systems to reduce fossil fuel consumption in Bologna. Also, as a city that has a moderate density of old buildings and modern architecture, and reasonable annual sunshine hours, Bologna is representative of many European cities, such as Barcelona and Prague. As such, results and findings obtained from Bologna have reference significance to other cities on the feasibility of promoting PV generation to meet the real electricity demand. Motivated by this, this study investigated the proposed PV installation optimization framework in Bologna.

Since equipping PV modules on characteristic historical buildings is not appropriate, the study focuses on a 3.05 km² urban area next to the old city center (Fig. 3), which is a typical residential area with a reasonable density of buildings compared with metropolises. There are 3761 buildings with a total floor area of 705,669 m², which is significantly larger than what was investigated in previous studies [13]. For ease of computation and statistics, the study defined 3D point clouds at 1 m resolution, which means that a single point represents 1 m², resulting in 5.46 million point clouds for the entire area.

3.2. Data collection

Electricity consumption data in April of 2019 was obtained from an anonymized data provider. The data was collected by *residential* smart meters and contains power consumption data at a temporal resolution of 15 min. For privacy protection, electricity consumption data has been aggregated by homogeneous and spatial contiguous grid-based regions at a resolution of 356 m, recorded as $g_{no} = \{1, 2, \dots, 17\}$ (Fig. 3). The study does not consider the impact of terrain variation on the spatial distribution of solar irradiations since the study area is mostly flat. We obtained footprints of the buildings associated with the height

Table 2

Comparison between the electricity generation on three partitions and real demand of the total electricity for four weeks.

| No. | Type | Electricity (GWh) |
|-----|----------|-------------------|
| 1 | Rooftops | 12.258451 |
| 2 | Facades | 18.972891 |
| 3 | Ground | 6.751774 |
| 4 | Total | 37.983116 |
| 5 | Demand | 1.575603 |

attribute from the Territorial Information System, the Municipality of Bologna [51]. Based on time t and location l , an online platform named Sun Earth Tools was used to compute the elevation angle e and azimuth z to compute solar irradiation r [52]. Since cloud cover is one of the most important factors that influence u significantly, hourly cloud-cover data in April has been collected for five years between 2015 and 2019 from World Weather Online [53], which is used to compute statistically significant transmittivity α and diffuse proportion β that significantly determine direct and diffuse solar irradiation [54]. With a determined $(e, z, \alpha, \beta, l, t)$, the irradiation u on a horizontal urban surface was computed by using Points Solar Radiation in ArcGIS 10.3 [55]. On this basis, a complete profile of land surface solar irradiation associated with time, location, and the weather was constructed and used by the 3D solar irradiation model. Eclipse Java IDE was utilized to connect and manage a series of databases simultaneously for parallel computation.

4. Results

4.1. Characterizing electricity supply and demand

Assuming that transition efficiency of PV modules is 20%, which has been widely achieved by industry [13]. The study computed hourly

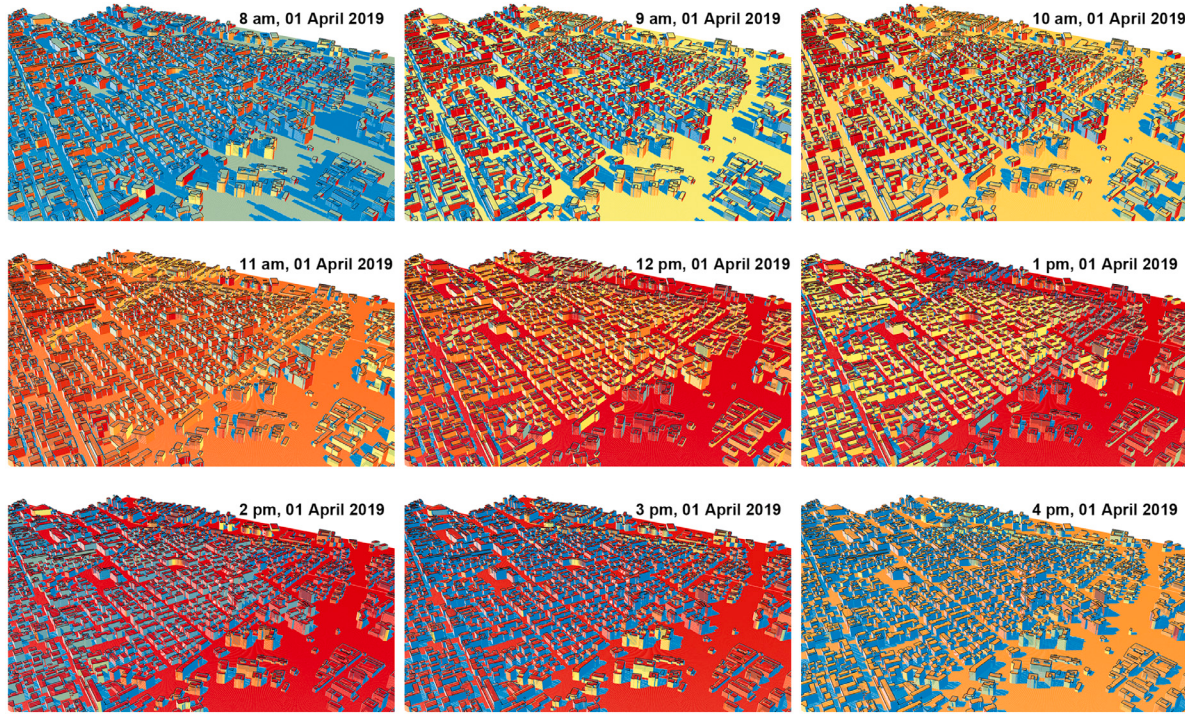


Fig. 4. Hourly solar irradiation on urban envelopes from 8 am to 4 pm on April 01, 2019.

solar irradiations on urban envelopes during the daytime. Fig. 4 visualizes the distribution of irradiation from 8 am to 4 pm on a single day. Based on the results on each day, we accumulated irradiations of 3D point clouds having the same spatial location across four weeks from 01 April 2019 to 28 April 2019. As a result of this, spatial analysis can be made based on a series of temporal scales from hours to days and even weeks.

The first question to address is whether the study area has enough solar capacity to satisfy the actual electricity demand. The study firstly overviews the whole area to draw a preliminary relation between supply and demand. We only consider land use types which are parks and grass when accumulating generated electricity on the ground as it is a challenge to use other land-use types for PV modules, such as schools or hospitals (Fig. 3). The analysis shows that the real demand is about 1.58 GWh versus the totally generated electricity is nearly 37.98 GWh in April, contributed by rooftops at 12.26 GWh, façades at 18.97 GWh, and ground at 6.75 GWh (Table 2). This means that, in principle, the study area has far enough solar capacity to supply the residential electricity demand, with a ratio between theoretical energy supply of demand of about 24x, and a ratio of about 7.8x considering only rooftop generation. However, the result of the analysis does not mean that people can utilize all the solar capacity. In fact, equipping PV modules on urban envelopes is usually constrained by many factors. For example, a surface with spatially concentrating and quantitatively large solar irradiation is always preferred for PV modules, while a surface having an opposite condition will be discarded probably.

4.2. Spatial distribution of solar irradiation

Then, the study summarized $p(r)$, which is an empirically cumulative distribution of rooftops such that each rooftop has at least a certain percentage of area $p(a)$ with irradiation at least $x \cdot u_m$ ($x = \{0.1, 0.2, \dots, 0.9\}$). For example, when looking at the blue curve in Fig. 5a, $p(r) = 0.7$ and $p(a) = 0.2$ mean that, for 70% rooftops, each rooftop has at least 20% area with irradiation $u \geq 0.9u_m$. The same statistics is also made for rates of ground $p(g)$ (Fig. 5b) and rates of façades $p(f)$ (Fig. 5c).

The results show that rooftops and ground have a similar distribution pattern, which has the largest rate of surface area ($p(a) = 1$) followed by a shape decrease and finally reaches the smallest rate ($p(a) = 0$) with the increase of $p(r)$ or $p(g)$. In detail, $p(r)$ experiences a steeper decrease than $p(g)$, suggesting that rooftops tend to be in sunshine or shadow alternatively while the ground has gradual changes between sunshine and shadow during the daytime. This also indicates that most rooftops are unlikely in the long-term shadow made by neighborhood buildings since there is no high density of tall buildings. Besides, more than 50% rooftops versus 40% ground can use 80% surface area respectively if targeting at the largest solar irradiation ($u \geq 0.9u_m$). In this aspect, rooftops may be more favorable than the ground to equip PV modules when only considering the spatial distribution of solar irradiations. In comparison, façades have a significantly different distribution pattern. For all $x \cdot u_m$, $p(a)$ has a dramatic or even cliff fall followed by a long tail approaching 0 with the increase of $p(f)$. This means that façades do not have large rates of surface area to utilize when $u \geq 0.9u_m$.

4.3. Quantitative distribution of the generated electricity

To determine usable areas of PV modules, the study makes absolute statistics and analysis as shown in Fig. 6. Overall, with the increase of x which is the rate of u_m , the total usable area $s(a)$ and the total generated electricity $s(e)$ decrease while the average electricity $v(e)$ increases for all rooftops, façades, and ground. Several observations can be derived from the figure. First, rooftops obtain relatively larger values than the ground at the same rate of u_m for all the considered statistics, suggesting that rooftops may have higher priority to use solar energy. Second, façades have the largest variation of $v(e)$, increasing from the smallest 16.8 KWh/m² when $x = 0.1$ to the significantly largest 38.7 KWh/m² when $x = 0.9$ (Fig. 6c). Even though façades do not have an advantage in the rate of the usable area if utilizing $u \geq 0.9u_m$ (Fig. 5c), the absolute statistics shows that façades still have a considerable usable area for $u \geq 0.9u_m$ (Fig. 6a), meaning that façades can be the best urban envelopes to use solar energy. Third, the analysis of $s(e)$ shows that we can meet the total residential energy demand when utilizing the largest irradiation when $x = 0.9$ (Fig. 6b), based on the fact that the real demand is at 1.58 GWh (Table 2).

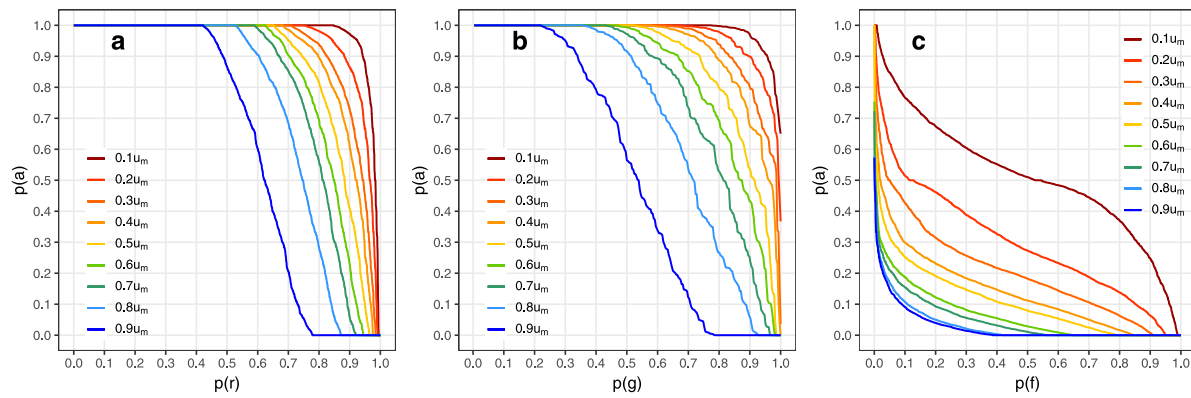


Fig. 5. A rate of surface area $p(a)$ in a rate of urban envelopes has solar irradiations equal or higher than $x \cdot u_m$. (a) Rate of rooftops $p(r)$. (b) Rate of ground $p(g)$. (c) Rate of façades $p(f)$.

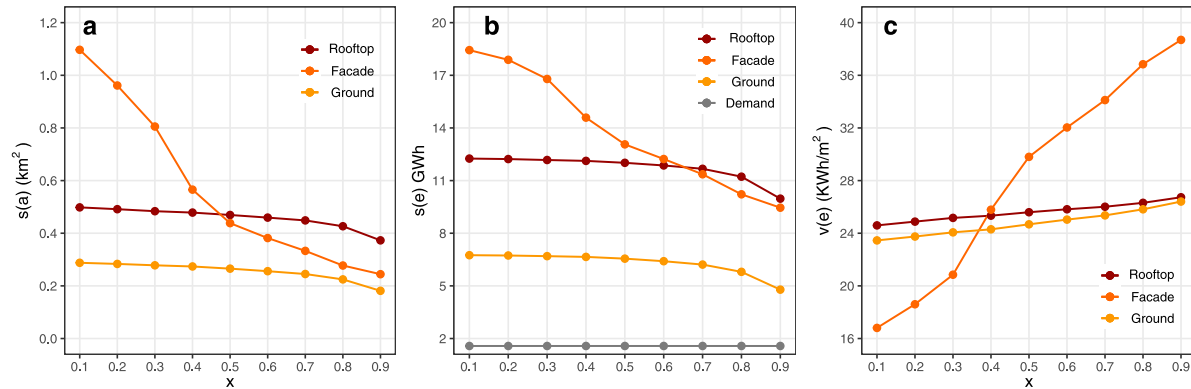


Fig. 6. Absolute statistics of solar irradiations when utilizing x rate of the maximum irradiation u_m on rooftops, façades, and ground. (a) The total usable area $s(a)$. (b) The total generated electricity $s(e)$. (c) The average electricity $v(e)$.

4.4. Planning of the PV capacities

Having obtained a thorough understanding of the spatial and quantitative distribution of solar energy on urban envelopes, our next focus is to propose an executable plan for deploying distributed PV modules for distributed energy production. Since large solar irradiation is always preferred, the results shown in Fig. 6 suggest that it is reasonable to utilize urban envelopes in order of façades, rooftops, and ground. However, Bologna is a historic city with a rich architectural landscape, and extensive use of building surfaces may destroy the original architecture landscape as the study area is just next to the old city center. Since the prevalent use of ground areas for PV modules may still be a challenge if the occupation of the ground is significant, we try to achieve a trade-off in which rooftops, ground, and façades are used with decreasing priority.

This study focuses on areas of high irradiation ($u \geq 0.9u_m$) as Section 4.3 has suggested that utilizing areas of high irradiation is sufficient to generate enough electricity to satisfy the residential energy demand. Therefore, Fig. 7 presents the energy production as a function of the minimum area a needed to install PV modules when $x \geq 0.9$, categorized by three urban partitions. Correspondingly, Fig. 8 reports the same analysis for the total area $s(a)$ that will be used for deploying PV modules. In general, with an increase in the minimum usable area a , both $s(e)$ and $s(a)$ drop off at a faster pace changing from ground to rooftops and façades. It also shows that each partition will get a larger $s(e)$ if we accept to use a smaller a on a single surface, which also means that the usable area may be spatially discrete, making it difficult to install and maintain PV modules.

As discussed above, the use of a single partition may already satisfy the current need since the real demand is 1.575603 GWh. Furthermore,

Table 3

Three plans of generating electricity on urban partitions. The bracketed numbers following the values of $s(e)$ are the corresponding rates x of u_m .

| No. | Partition | a (m^2) | $s(e)$ (GWh) | $s(a)$ (m^2) | $p(a)$ |
|-----|-----------|----------------------|-----------------|-------------------------|----------|
| P1 | Façade | 50 | 1.968919 (0.93) | 36 269 | 2.0464% |
| P2 | Rooftop | 500 | 2.106683 (0.98) | 77 347 | 15.3796% |
| P3 | Ground | 500 | 1.756860 (0.98) | 64 697 | 3.9172% |

the study plans to generate electricity that fulfills the real demand with the smallest occupation of urban surfaces, which can simultaneously determine the rate of u_m . If utilizing façades that have the largest solar irradiation, it can generate electricity at 1.968919 WKwh ($u \geq 0.93u_m$), which corresponds to a total area of 36,269 m^2 for the PV modules (Table 3). To protect the original architectural landscape, free space on the ground can be used to generate electricity at 1.756860 GWh ($u \geq 0.98u_m$). Even though the generated electricity is only slightly less than façades, the required area of PV modules is significantly larger, requiring 64,697 m^2 . As a trade-off, we may alternatively install PV modules on rooftops with at least 500 m^2 to meet the condition ($u \geq 0.98u_m$). In this scenario, the system would be able to distributedly generate a large amount of electricity at 2.1066883 GWh, using a total area of 77,347 m^2 for PV modules. Overall, 2.0464%, 15.3796%, and 3.9172% of the total façade, rooftop, and ground surface will be occupied by PV modules, respectively.

4.5. Spatio-temporal constraints of the PV modules

The above analysis shows that we can generate enough electricity to meet residential electricity demand with the least occupation of the

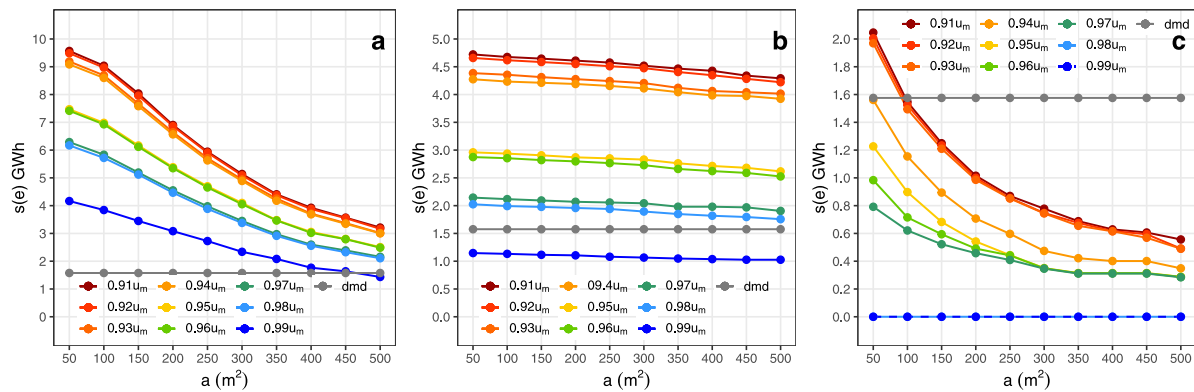


Fig. 7. The minimum usable area (a) in each urban partition against the totally generated electricity ($s(e)$), varying by the use of the minimum irradiation $u \geq x \cdot u_m$, where $x = \{0.91, 0.92, \dots, 0.99\}$. (a) $s(e)$ on rooftops. (b) $s(e)$ on ground. (c) $s(e)$ on façades.

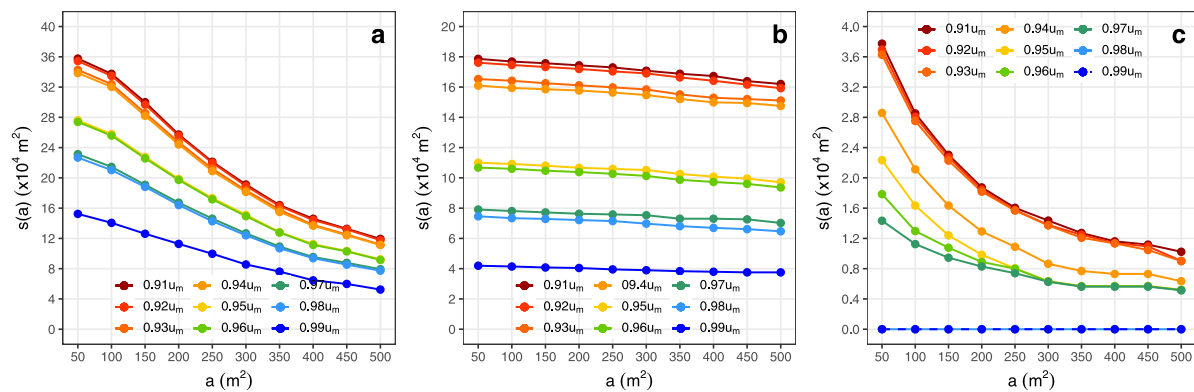


Fig. 8. The minimum usable area (a) in each urban partition against the total required area ($s(a)$), varying by the use of the minimum irradiation $u \geq x u_m$, where $x = \{0.91, 0.92, \dots, 0.99\}$. (a) $s(a)$ on rooftops. (b) $s(a)$ on ground. (c) $s(a)$ on façades.

Table 4

Combination of generating electricity on three urban partitions based on different concerns. Values afflicted with the “+” mark means that the generated electricity exceeds the demanded electricity.

| No. | $s(e)_{dmd}$ (GWh) | $s(e)_{p1}$ (GWh) | $s(e)_{p2}$ (GWh) | $s(e)_{p3}$ (GWh) |
|-----|--------------------|-----------------------|-----------------------|-----------------------|
| 1 | 0.047409 | 0.094445 ⁺ | 0.083220 ⁺ | 0 |
| 2 | 0.024669 | 0.175764 ⁺ | 0.120474 ⁺ | 0 |
| 3 | 0.155910 | 0.106263 | 0.093779 | 0 |
| 4 | 0.166313 | 0.064986 | 0.144812 | 0 |
| 5 | 0.011003 | 0.029369 ⁺ | 0.032090 ⁺ | 0.014928 ⁺ |
| 6 | 0.096165 | 0.280699 ⁺ | 0.022929 | 0.378268 ⁺ |
| 7 | 0.023208 | 0.119614 ⁺ | 0 | 1.177474 ⁺ |
| 8 | 0.070116 | 0.048545 | 0.154948 ⁺ | 0 |
| 9 | 0.105567 | 0.169071 ⁺ | 0.319250 ⁺ | 0 |
| 10 | 0.195715 | 0.059613 | 0.156334 | 0 |
| 11 | 0.230294 | 0.094655 | 0.050123 | 0.018667 |
| 12 | 0.083574 | 0.159877 ⁺ | 0.127141 ⁺ | 0.068493 |
| 13 | 0.048793 | 0.147488 ⁺ | 0.114729 ⁺ | 0 |
| 14 | 0.091564 | 0.101495 ⁺ | 0.125080 ⁺ | 0 |
| 15 | 0.127958 | 0.147461 ⁺ | 0.036702 | 0 |
| 16 | 0.075593 | 0.079560 ⁺ | 0.058173 | 0 |
| 17 | 0.021754 | 0.090013 ⁺ | 0.466901 ⁺ | 0.099029 ⁺ |

urban surface. However, there are still two uncertainties. When looking at spatial constraints, a grid-based statistical area may obtain a self-supportive energy balance; however, it can also be possible that some areas lack electricity while others have a surplus so that rebalance would be needed across the entire area. Having several grid areas with self-sufficient PV power generation is an indication of a relatively more resilient distributed PV system, as most of the areas of the city would be able to self-produce their energy in case of a break-down of the main power grid. Furthermore, when considering temporal constraints,

electricity generated during the daytime may or may not be able to supply electricity demand throughout a day in *real-time*. If this situation occurs, there is a need to install storage capacity to provide electricity during the night.

To account for both spatial and temporal constraints, the study compares generated electricity with the real demand in each of the statistical areas. It shows that 12 out of 17 (71%) areas have surplus electricity on façades (Table 4), which has the best self-supportive character. The reason is that the high electricity demand is likely associated with tall buildings, which also indicates large façades that can potentially generate a considerable amount of electricity. Even though façades in other areas might be insufficient to provide the required electricity, there is still a considerable amount of solar irradiation to be used to generate more electricity locally, which can achieve a self-supportive architecture. In comparison, rooftops have 9 areas (53%) and the ground has 4 areas (24%) that meet the real demand, respectively. Notably, the ground has only four self-supportive areas, even though the four areas can generate far enough electricity to satisfy the local demand. However, several areas cannot generate electricity. This suggests that, if deploying PV modules on rooftops or ground, load balancing between the areas is needed. This will require interfacing the distributed PV solar system with the local power grid to redistribute energy across the study area.

Spatial visualization verifies the statistics in Table 3 that PV modules will occupy a small proportion of the surface, and utilization of the façades mainly concentrates in an upper level with a southeast orientation (Fig. 9a). In detail, utilized façades (Fig. 9b) and rooftops (Fig. 9c, d) have contiguously large area with some parts abandoned. This suggests the effectiveness of the model in two aspects: (i) area with irradiation interrupted by nearby buildings will not be used, and (ii) the model is not “near-sighted” at an instant of time but counts

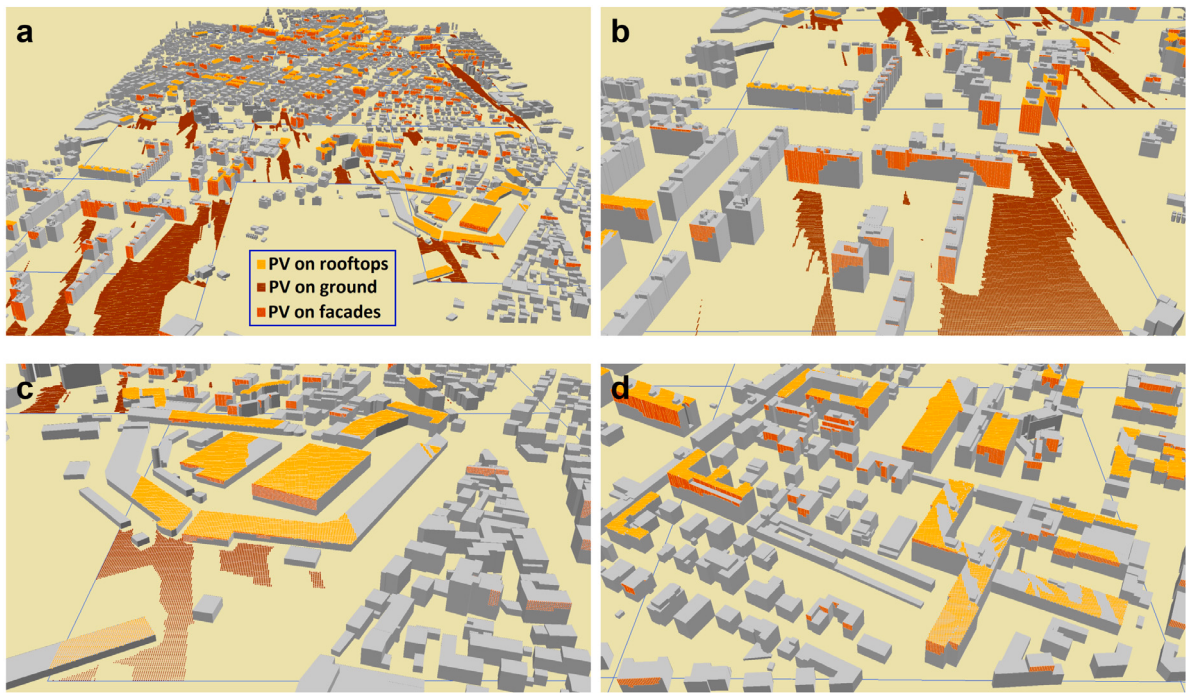


Fig. 9. Spatial location of planned PV modules in three different plans is presented by 3D point clouds. Location of the grid number (g_{no}) corresponds to the presentation in Fig. 3. (a) Overview of the study area. (b) Area at $g_{no} = \{7\}$. (c) Area at $g_{no} = \{17\}$. (d) Area at $g_{no} = \{9\}$.

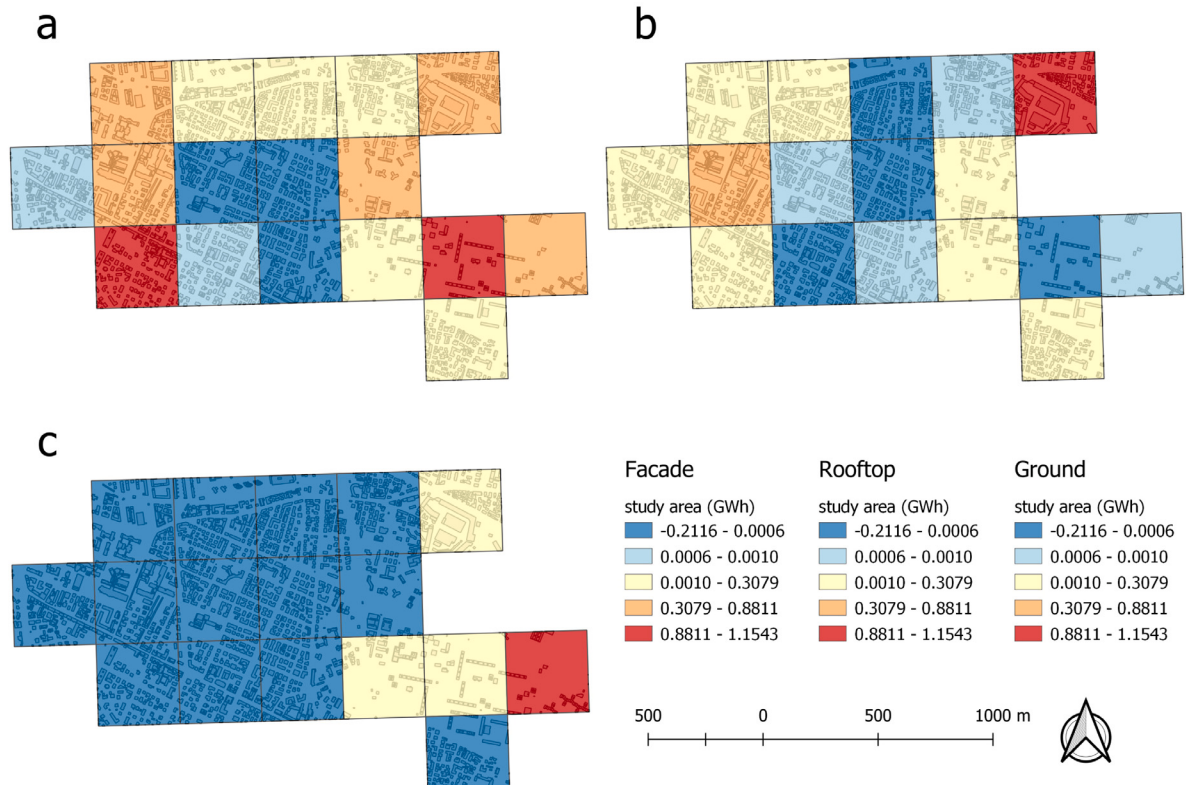


Fig. 10. Grid-based areas with different colors corresponding to whether each region is self-sufficient. Positive values mean self-sufficient versus negative values mean self-insufficient. (a) Façades. (b) Rooftops. (c) Ground.

the accumulative intensity over a long period. Besides, the use of ground is rather limited in a dense residential area due to the land use constraint (Fig. 9d). The study also investigates whether each grid-based area is self-sufficient by simply calculating the difference

between the generated and consumed electricity (Fig. 10). It reveals that four spatial contiguous regions with a high density of buildings ($g_{no} = \{3, 4, 10, 11\}$) are insufficient versus two regions ($g_{no} = \{5, 17\}$) are sufficient in all the three plans.

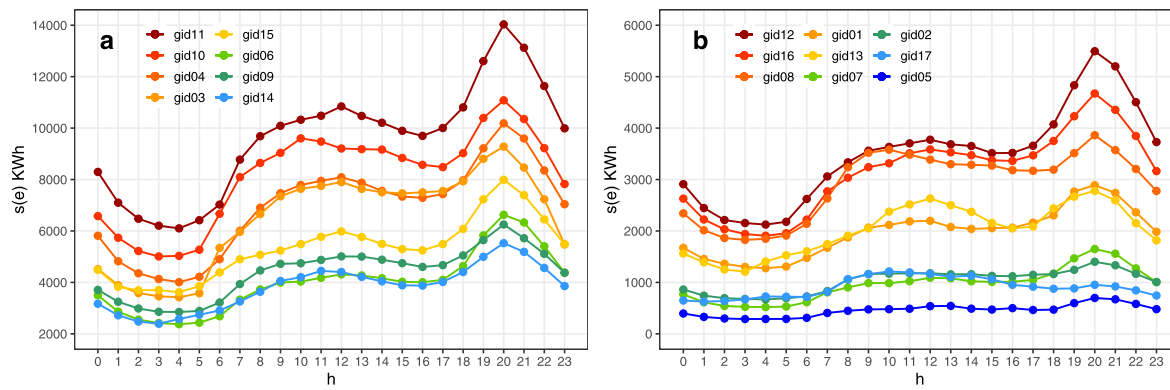


Fig. 11. Accumulation of hourly demand electricity $s(e)$ in the 17 statistical areas for four weeks in April. (a) Eight large $s(e)$. (b) Nine small $s(e)$.

Furthermore, the study plots the accumulation of hourly consumed electricity for the seventeen areas for the four weeks in April (Fig. 11). Overall, the use of the electricity increases from 4 am till 12 pm followed by a slight decrease till 4 pm; then, it experiences the second and steep growth approaching the largest consumption at 9 pm with the other decrease till 4 am in the next day. Specifically, the total amounts vary significantly among different statistical areas. Besides, the largest two curves associate with the hospitals and high density of buildings while the smallest two have a large area of parks and grass. To the best of our knowledge, the revealed trends are consistent with the electricity consumption of residents' daily schedule, with a possible variation made by service buildings, such as hospitals.

In a more aggregate investigation of the entire area, we draw the curves of hourly generated electricity on three urban partitions that correspond to the three proposed plans and the curve of hourly electricity consumption (Fig. 12). It shows that rooftops generate more electricity than ground with a similar and smooth curve, which can supply the demand in *real-time* in the daytime. In comparison, the vast majority of the generated electricity on façades concentrates in the early morning following a sharp decrease that the electricity becomes quite small after 1 pm. There are two major reasons. First, the elevation is rather small in the early morning in April that makes solar irradiation large on façades. Second, it makes the accumulation process significant at a considerably large amount as a large area of façades is solar-facing orientated in the morning. To sum up, each plan can fully or partially supply the demand in the daytime but it cannot support peak hours during the night without storage capacity. This means that additional measures are needed in any scenario if aiming at a self-supportive distributed solar energy system throughout the day.

5. Discussion and conclusion

This study proposes a hierarchical PV capacity optimization framework that maximizes the distributed solar farming and minimizes the total PV area to meet real electricity demand. The finding shows that façades have the largest solar PV installation capacity in Bologna, followed by rooftops and ground, which is possible to support household electricity demand. The estimated results are reliable and accurate because the framework has modeled the physical effects from extraterrestrial solar irradiation determined by an instant of time and the location of the city, historical atmospheric conditions, and shadow created by all the buildings.

This study achieves a global optimization for the site selection of the PV modules across the entire study area. The proposed computational optimization is crucial to this accomplishment because it enables spatially scalable parallel computation for a large urban area while removing marginal effects on the solar potential. However, there is a

trade-off that storage facilities and rebalance are needed to deal with the mismatch between demand and supply in sub-areas. Alternatively, a local optimization can be performed, which plans the PV installation capacity based on each independent sub-area, resulting in a simple operation of the smart grid. This implies that the proposed optimization framework can be used for PV planning in various scenarios.

The impact of this study is beyond simply generating a large amount of green electricity when occupying a small proportion of the urban surface. The proposed PV capacity optimization can be used to facilitate energy transition in many fields, making broader social and economic impacts. For instance, it has been suggested that PV charging platforms can reduce extensive manpower to frequently recycling, charging, and repositioning the shared electric scooters, leading to a significant reduction of the operational cost [56]. By using the proposed optimization method, the PV location, size, and installation layout can be customized for each charging station to improve the overall operational efficiency of the whole mobility sharing service.

It is also important to observe that the proposed PV installation optimization is helpful to develop an economically feasible PV power generation system. To compete with local electricity prices, the smallest occupation of urban surfaces obtained from this study is critical, which can minimize the cost of purchasing, installing, and maintaining PV modules. When the proposed PV optimization is incorporated into a techno-economic assessment model to ensure the energy cost is less than the local electricity price, the distributed PV systems will have a significant impact on facilitating the energy transition from fossil-based to zero-carbon electricity generation to meet the carbon neutrality target [57].

It is worth noting that there are two uncertainties. First, this study assumes that all rooftops are horizontal. For tilted rooftops with solar-facing and back-shadow surfaces, even though the spatial distribution of solar PV potential is heterogeneous on each rooftop, the total solar PV potential is determined. Note that the solar estimation model used in this study can estimate this spatial heterogeneity for microscale planning of PV installation when the data set with structured rooftops is provided. Second, due to the scarcity of electricity demand data, the optimization is limited to one month in April. Further research may be required to modify the planned PV size and location based on changes in electricity demand, solar trajectory, and atmospheric conditions for PV optimization over the entire year. Since Bologna has a mid-latitude and humid subtropical climate, it has larger solar irradiation and much less cloud cover from April to September, suggesting that the planned PV modules will generate more electricity during this period. In contrast, it will generate deficient electricity from October to the next March if the electricity demand remains constant.

To conclude, the proposed PV optimization framework is effective to support real electricity demand in Bologna, accounting for the constraints of preserving the city's architectural landscape and conserving

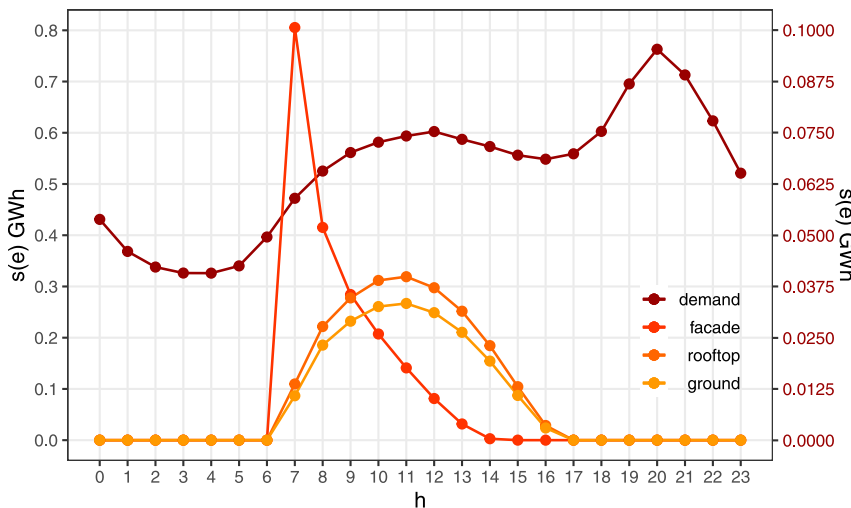


Fig. 12. Accumulation of hourly generated electricity $s(e)$ (the left y-axis) and the real demand $s(e)$ (the right y-axis) for the whole study area over four weeks in April.

valuable urban land. For global PV optimization across the entire study area, electricity storage and rebalance are usually needed for building an independent smart grid. There is a great potential to promote distributed PV systems in other cities similar to Bologna. The framework is generic and adaptable, which can be applied to a variety of applications to facilitate the energy transition.

CRediT authorship contribution statement

Rui Zhu: Methodology, Investigation, Formal analysis, Writing – original draft, Writing – review & editing. **Cheng Cheng:** Formal analysis, Validation, Writing – original draft. **Paolo Santi:** Conceptualization, Methodology, Writing – review & editing. **Min Chen:** Investigation, Visualization. **Xiaohu Zhang:** Investigation, Visualization. **Martina Mazzarello:** Data collection and data editing. **Man Sing Wong:** Conceptualization, Writing – review & editing, Supervision. **Carlo Ratti:** Conceptualization, Writing – review & editing, Supervision.

Declaration of competing interest

The authors declare that they have no known competing financial interests or personal relationships that could have appeared to influence the work reported in this paper.

Acknowledgments

This research is supported by (i) the National Research Foundation, Singapore under its Campus for Research Excellence and Technological Enterprise (CREATE) programme, Prime Minister's Office, Singapore, (ii) the Enel Foundation, Italy, (iii) the Strategic Hiring Scheme (Grant No. P0036221) at Thong Kong Polytechnic University, and (iv) the General Research Fund (Grant No. 15602619 and 15603920) and Collaborative Research Fund (Grant No. C5062-21GF), the Hong Kong Research Grant Council, Hong Kong, China.

References

- [1] United Nations. UN-habitat strategic plan 2020–2023. 2022, https://unhabitat.org/sites/default/files/documents/2019-09/strategic_plan_2020-2023.pdf [Accessed 3 March 2022].
- [2] Kan Z, Wong MS, Zhu R. Understanding space-time patterns of vehicular emission flows in urban areas using geospatial technique. *Comput Environ Urban Syst* 2020;79:101399.
- [3] Masson V, Bonhomme M, Salagnac JL, Briottet X, Lemonsu A. Solar panels reduce both global warming and urban heat island. *Front Environ Sci* 2014;2:14.
- [4] Zhu R, Guibert E, Wong MS. Object-oriented tracking of spatial and thematic dynamic behaviors of urban heat islands. *Trans GIS* 2020;24:85–103.
- [5] Zhu R, Guibert E, Wong MS. Object-oriented tracking of the dynamic behavior of urban heat islands. *Int J Geogr Inf Sci* 2017;31(2):405–24.
- [6] Zhu R, Wong MS, Guibert E, Chan PW. Understanding heat patterns produced by vehicular flows in urban areas. *Sci Rep* 2017;7:16309.
- [7] Chu S, Majumdar A. Opportunities and challenges for a sustainable energy future. *Nature* 2012;488:294–303.
- [8] Ma S, Goldstein M, Pitman AJ, Haghadi N, MacGill I. Pricing the urban cooling benefits of solar panel deployment in Sydney, Australia. *Sci Rep* 2017;7:43938.
- [9] Molina A, Falvey M, Rondanelli R. A solar radiation database for Chile. *Sci Rep* 2017;7:14823.
- [10] Ogbonnaya C, Abeykoon C, Damoa UM, Turana A. The current and emerging renewable energy technologies for power generation in Nigeria: A review. *Therm Sci Eng Prog* 2019;13:100390.
- [11] Meyers S, Schmitt B, Vajen K. Renewable process heat from solar thermal and photovoltaics: The development and application of a universal methodology to determine the more economical technology. *Appl Energy* 2018;212:1537–52.
- [12] Baum Z, Palatnik RR, Ayalon O, Elmakis D, Frant S. Harnessing households to mitigate renewables intermittency in the smart grid. *Renew Energy* 2019;132:1216–29.
- [13] Zhu R, Wong MS, Kwan MP, Chen M, Santi P, Ratti C. An economically feasible optimization of photovoltaic provision using real electricity demand: A case study in New York city. *Sustainable Cities Soc* 2022;78:103614.
- [14] Kettani M, Bandelier P. Techno-economic assessment of solar energy coupling with large-scale desalination plant: The case of Morocco. *Desalination* 2020;494:114627.
- [15] Oh J, Koo C, Hong T, Cha SH. An integrated model for estimating the techno-economic performance of the distributed solar generation system on building façades: Focused on energy demand and supply. *Appl Energy* 2018;228:1071–90.
- [16] Savvides A, Vassiliades C, Michael A, Kalogirou S. Siting and building-massing considerations for the urban integration of active solar energy systems. *Renew Energy* 2019;135:963–74.
- [17] Kanteris J, Wall M, Dubois MC. Typical values for active solar energy in urban planning. *Energy Procedia* 2014;48:1607–16.
- [18] Lobaccaro G, Frontini F. Solar energy in urban environment: how urban densification affects existing buildings. *Energy Procedia* 2014;48:1559–69.
- [19] Morganti M, Salvati A, Coch H, Cecere C. Urban morphology indicators for solar energy analysis. *Energy Procedia* 2017;134:807–14.
- [20] Heo J, Jung J, Kim B, Han S. Digital elevation model-based convolutional neural network modeling for searching of high solar energy regions. *Appl Energy* 2020;262:114588.
- [21] Calcabrini A, Ziar H, Isabella O, Zeman MA. Simplified skyline-based method for estimating the annual solar energy potential in urban environments. *Nat Energy* 2019;4:2058–7546.
- [22] Jakubiec JA, Reinhart CF. A method for predicting city-wide electricity gains from photovoltaic panels based on LiDAR and GIS data combined with hourly daysim simulations. *Sol Energy* 2013;93:127–43.
- [23] Li Y, Ding D, Liu C, Wang C. A pixel-based approach to estimation of solar energy potential on building roofs. *Energy Build* 2016;129:563–73.
- [24] Wong MS, Zhu R, Liu Z, Lu L, Peng J, Tang Z, Lo CH, Chan WK. Estimation of Hong Kong's solar energy potential using GIS and remote sensing technologies. *Renew Energy* 2016;99:325–35.
- [25] Catita C, Redweik P, Pereira J, Brito MC. Extending solar potential analysis in buildings to vertical facades. *Comput Geosci* 2014;66:1–12.

- [26] Redweik P, Catita C, Brito M. Solar energy potential on roofs and facades in an urban landscape. *Sol Energy* 2013;97:332–41.
- [27] Liang J, Gong J, Li W, Ibrahim AN. A visualization-oriented 3D method for efficient computation of urban solar radiation based on 3D–2D surface mapping. *Int J Geogr Inf Sci* 2014;28(4):780–98.
- [28] Liang J, Gong J, Zhou J, Ibrahim AN, Li M. An open-source 3D solar radiation model integrated with a 3D geographic information system. *Environ Model Softw* 2015;64:94–101.
- [29] Chatzipoulka C, Compagnon R, Nikolopoulou M. Urban geometry and solar availability on facades and ground of real urban forms: using London as a case study. *Sol Energy* 2016;138:53–66.
- [30] Zhu R, Wong MS, You L, Santi P, Nichol J, Ho HC, Lu L, Ratti C. The effect of urban morphology on the solar capacity of three-dimensional cities. *Renew Energy* 2020;153:1111–26.
- [31] Zhu R, You L, Santi P, Wong WS, Ratti C. Transformation of solar accessibility in reforming urban areas: A case study in Kowloon east, Hong Kong. *Sustainable Cities Soc* 2019;51:101738.
- [32] Li P, Zhang H, Gue Z, Lyu S, Chen J, Li W, Song X, Shibusaki R, Yan J. Understanding rooftop PV panel semantic segmentation of satellite and aerial images for better using machine learning. *Adv Appl Energy* 2021;4:100057.
- [33] Amado M, Poggi F. Solar urban planning: a parametric approach. *Energy Procedia* 2014;48:1539–48.
- [34] Amado M, Poggi F, Amado AR. Energy efficient city: A model for urban planning. *Sustainable Cities Soc* 2016;26:476–85.
- [35] Vakilifard N, Bahri PA, Anda M, Ho G. An interactive planning model for sustainable urban water and energy supply. *Appl Energy* 2019;235:332–45.
- [36] Polo Lépeza CS, Salab M, Tagliabuec LC, Frontinia F, Bouziri S. Solar radiation and daylighting assessment using the sky-view factor (SVF) analysis as method to evaluate urban planning densification policies impacts. *Energy Procedia* 2016;91:989–96.
- [37] Gong FY, Zeng ZC, Ng E, Norford LK. Spatiotemporal patterns of street-level solar radiation estimated using google street view in a high-density urban environment. *Built Environ* 2019;148:547–66.
- [38] Jing R, Wang X, Zhao Y, Zhou Y, Wu J, Lin J. Planning urban energy systems adapting to extreme weather. *Adv Appl Energy* 2021;3:10005.
- [39] Lindberg F, Jonsson P, Honjo T, Wästberg D. Solar energy on building envelopes – 3D modelling in a 2D environment. *Sol Energy* 2015;115:369–78.
- [40] Lobaccaro G, Carlucci S, Croce S, Paparella R, Finocchiaro L. Boosting solar accessibility and potential of urban districts in the nordic climate: A case study in trondheim. *Sol Energy* 2017;149:347–69.
- [41] Erdélyi R, Wang Y, Guo W, Hanna E, Colantuono G. Three-dimensional solar radiation model (SORAM) and its application to 3-D urban planning. *Sol Energy* 2014;101:63–73.
- [42] Hofierka J, Zlocha M. A new 3-D solar radiation model for 3-D city models. *Trans GIS* 2012;16(5):681–90.
- [43] Perez R, Ineichen P, Seals R, Michalsky J, Stewart R. Modeling daylight availability and irradiance components from direct and global irradiance. *Sol Energy* 1990;44(5):271–89.
- [44] Peronato G, Rey E, Andersen M. 3D model discretization in assessing urban solar potential: the effect of grid spacing on predicted solar irradiation. *Sol Energy* 2018;176:334–49.
- [45] Bianchi M, Branchini L, Ferrari C, Melino F. Optimal sizing of grid-independent hybrid photovoltaic–battery power systems for household sector. *Appl Energy* 2014;136:805–16.
- [46] Zhang J, Xua L, Shabunko V, Tay SER, Sun H, Lau SSY, Reindl T. Impact of urban block typology on building solar potential and energy use efficiency in tropical high-density city. *Appl Energy* 2019;240:513–33.
- [47] Dasari HP, Desamsetti S, Langdon S, Attada R, Kunchala RK, Viswanadhapalli Y, Knio O, Hoteit I. High-resolution assessment of solar energy resources over the Arabian peninsula. *Appl Energy* 2019;248:354–71.
- [48] Perera ATD, Javanroodi K, Wang Y, Hong T. Urban cells: Extending the energy hub concept to facilitate sector and spatial coupling. *Adv Appl Energy* 2021;3:100046.
- [49] Giovanardi M, Silvagni MG. Profiling ‘Red Bologna’: Between neoliberalisation tendencies and municipal socialist legacy. *Cities* 2021;110:103059.
- [50] Melica G. The covenant of mayors initiative for local sustainable energy. 2020, <https://e3p.jrc.ec.europa.eu/node/188> [Accessed 3 March 2022].
- [51] Municipality of Bologna. Urban planning and construction. 2021, <http://dru.iperbole.bologna.it/pianificazione> [Accessed 3 March 2022].
- [52] Sun Earth Tools. Tools for consumers and designers of solar. 2021, https://www.sunearthtools.com/dp/tools/pos_sun.php?lang=en [Accessed 3 March 2022].
- [53] World Weather Online. Historical monthly weather. 2021, <https://www.worldweatheronline.com> [Accessed 11 October 2021].
- [54] Huang S, Rich PM, Crabtree R, Potter C. Modeling monthly near-surface air temperature from solar radiation and lapse rate: Application over complex terrain in yellowstone national park. *Phys Geogr* 2008;29(2):158–78.
- [55] ArcGIS for Desktop. Points solar radiation. 2021, <http://desktop.arcgis.com/en/arcmap/10.3/tools/spatial-analyst-toolbox/points-solar-radiation.htm> [Accessed 3 March 2022].
- [56] Zhu R, Kondor D, Cheng C, Zhang X, Santi P, Wong MS, Rattis C. Solar photovoltaic generation for charging shared electric scooters. *Appl Energy* 2022;313:118728.
- [57] Yan J. Energy transition: Time matters. *Adv Appl Energy* 2022;5:100082.